China Ocean Eng., Vol. 29, No. 1, pp. 49 – 64

DOI 10.1007/s13344-015-0004-4, ISSN 0890-5487

An Analytical Method for Positioning Drag Anchors in Seabed Soils*

ZHANG Wei (张 炜)[a, 1], LIU Hai-xiao (刘海笑)[b], LI Xin-zhong (李新仲)[a],
LI Qing-ping (李清平)[a] and CAO Jing (曹 静)[a]

[a] *General Research Institute*, *China National Offshore Oil Corporation*, *Beijing 100027*, *China*
[b] *School of Civil Engineering*, *Tianjin University*, *Tianjin 300072*, *China*

(Received 6 March 2013; received revised form 25 June 2013; accepted 31 October 2013)

ABSTRACT

Positioning drag anchors in seabed soils are strongly influenced not only by the properties of the anchor and soil, but also by the characteristics of the installation line. The investigation on the previous prediction methods related to anchor positioning demonstrates that the prediction of the anchor position during dragging has inevitably introduced some key and unsubstantiated hypotheses and the applicability of these methods is limited. In the present study, the interactional system between the drag anchor and installation line is firstly introduced for the analysis of anchor positioning. Based on the two mechanical models for embedded lines and drag anchors, the positioning equations for drag anchors have been derived both for cohesive and noncohesive soils. Since the drag angle at the shackle is the most important parameter in the positioning equations, a novel analytical method that can predict both the variation and the exact value of the drag angle at the shackle is proposed. The analytical method for positioning drag anchors which combines the interactional system between the drag anchor and the installation line has provided a reasonable theoretic approach to investigate the anchor behaviors in soils. By comparing with the model flume experiments, the sensitivity, effectiveness and veracity of the positioning method are well verified.

Key words: *drag anchor*; *anchor positioning*; *mechanical model*; *drag line*; *embedded line*; *drag angle*; *trajectory*

1. Introduction

Drag embedment plate anchor is an attractive option for deepwater mooring systems owing to its better performances both in the pullout capacity and the deepwater installation. It is well known that the positioning techniques for drag anchors are especially important because the anchor's working performance is closely related to the embedment depth, the anchor orientation, and the properties of the surrounding soils (Murff *et al*., 2005). However, predicting the position of drag anchors in seabed soils presents a significant challenge, largely because of the uncertainty in predicting the anchor trajectory during installation, which is strongly influenced not only by the properties of the anchor and soil, but also by the characteristics of the installation line. Further studying the positioning technique is a critical problem and two aspects should be included in, i.e., (1) what are the key parameters of the anchor positioning and the relationships among these parameters during the anchor embedment; (2) how to

* This paper was financially supported by the National Basic Research Program of China (973 Program, Grant No. 2009CB219507), the National Natural Science Foundation of China (Grant Nos. 50639030 and 50979070), and the National Science and Technology Major Project of China (Grant Nos. 2011ZX05056-002 and 2011ZX05026-004).
1 Corresponding author. E-mail: zw299@163.com

predict the exact position or kinematic trajectory of the anchor in seabed soils.

Drag embedment plate anchors, also called drag-in plate anchors or vertically loaded plate anchors (VLAs) elsewhere, are installed in the same way as the conventional drag anchors. Under the drag force transmitted from the installation line, the anchor gradually penetrates into the soil, as shown in Fig. 1. It can be observed that, during dragging, the embedment depth and the horizontal position of the anchor asymptotically increase; while inversely, the anchor orientation gradually decreases. Owing to the soil resistance, the embedded segment of the installation line takes on a reverse curvature and its shape becomes steeper during the embedment, such that the line imposes some vertical load components on the anchor. Because of the invisibility of seabed soils, both the configuration of the embedded segment of the installation line and the trajectory of the anchor are complicated and cannot be directly observed.

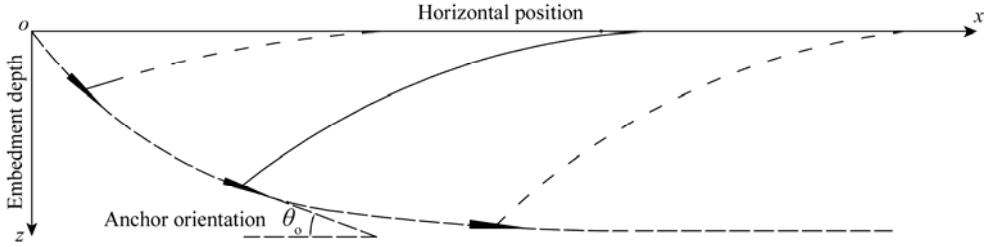

Fig. 1. Key parameters during the anchor penetration.

Positioning in seabed soils is still a great challenge to drag anchors. The offshore industry has largely relied on the empirical methods (e.g. Naval Civil Engineering Laboratory, 1987; Vryhof Anchors, 2005). Obviously, the empirical approaches are based on a large amount of test data and involve considerable uncertainties in extrapolating data with different soil conditions and anchor geometries. The positioning methods that can provide rational prediction of the anchor position need a numerical incremental computation, and generally fall into two groups, i.e., the limit equilibrium method and the plastic limit analysis method.

Various limit equilibrium methods proposed by many investigators (Dahlberg, 1998; Neubecker and Randolph, 1996a; Ruinen, 2004; Stewart, 1992; Thorne, 1998) provide a rational basis for the trajectory prediction of drag anchors. These methods are typically incremental ones based on an estimated distribution of soil resistances acting on the anchor under a failure condition, and the installation line mechanics can also be combined with the computational model. Plastic limit analysis methods adopted by a number of investigators (Aubeny *et al*., 2005, 2008; Kim, 2005; O'Neill *et al*., 2003) are in many ways similar to the limit equilibrium method. The major difference is that the plasticity concepts are used to determine the forces acting on the anchor whereas the associated plastic anchor displacements are used to determine the anchor kinematics.

Theoretical prediction methods are proposed only by two investigators for anchor positioning, namely Neubecker and Randolph (1996a) and Liu *et al*. (2012a). In the former literature, a closed-form expression that approximates the trajectory of a drag anchor was proposed. This expression was directly derived from the property that the anchor orientation parallels the tangent of the anchor trajectory by employing a simple equation which relates the drag angle and tension at the anchor shackle. However, it is only applicable to the clay that obeys the power law. In the later literature, a theoretical framework for

predicting the trajectory of drag anchors was established. It was derived on the basis of several key hypotheses, i.e., the drag angle to the fluke at the shackle keeps constant and the anchor moves parallel to its fluke, besides, the relation between the embedment depth and the drag angle to the horizontal at the shackle is assumed based on the boundary conditions of the anchor embedment. Obviously, all the hypotheses need to be further verified.

Hypothetical studies were reported by Murff *et al*. (2005), in which five organizations or individuals using their own methods contributed to the prediction exercise of the anchor position. From the review of the participants' results, it indicates that different predictors obtain different results and the deviations are significant. It can be found that there are still uncertainties in the positioning problem of drag anchors by using numerical incremental methods.

In the present study, a novel analytical method for positioning drag anchors in seabed soils is established. The method preferably utilizes the present understandings of the key parameters of the anchor penetration, introduces the interactional system between the drag anchor and the installation line, and allows a more thorough and reliable evaluation of the anchor position. Based on the mechanical models for the anchor and installation line, the anchor positioning equations, namely, the relationship between the embedment depth and the anchor orientation is derived. The drag angle at the shackle is the most important parameter in the positioning equations, and a novel analytical method that can predict both the variation and the exact value of the drag angle at the shackle during the anchor penetration is proposed. Subsequently, the model tests in saturated sand are employed to examine the sensitivity, effectiveness and veracity of the analytical model and theoretical framework for the anchor positioning.

2. Analytical Model for Predicting the Position of Drag Anchors

2.1 Basic Assumptions and Definitions

Basic assumptions are as follows:

(1) The AHV (anchor handling vessel), drag line and anchor all move in the same plane.

(2) The length of the drag line is long enough for the anchor to reach the ultimate embedment depth.

(3) The axial deformation and self-weight of the drag line are neglected.

(4) The side displacement and roll of the anchor are unconsidered.

It should be pointed out that, the first two assumptions can be easily ensured by installation techniques. Compared with the anchor movement in seabed soils, the effects induced by the axial deformation and self-weight of the drag line are inappreciable, and thus, the third assumption is also reasonable. During the anchor installation process, if the side displacement and roll of the anchor are remarkable, then the lateral stability of the anchor will be lost and the dragging process will be considered as a failure, and the last assumption will be reasonable.

Based on the second assumption, as demonstrated in Fig. 2, the segment of the installation line in the seawater is called the catenary line, the segment on the seafloor surface is called the horizontal line, and the segment embedded in soils, which presents a reverse curvature compared with the catenary line, is called the embedded line; the point of intersection between the anchor and the embedded line is called the shackle (or the attachment point) of the anchor; the point of intersection between the embedded line

and the horizontal line is defined as the embedment point.

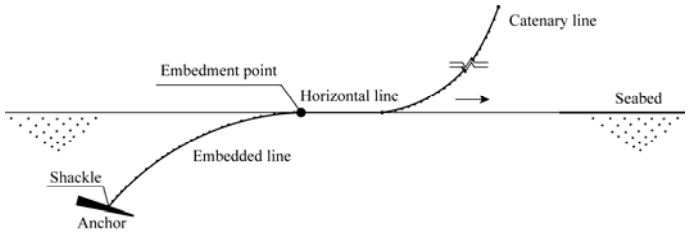

Fig. 2. Definition of the installation line.

2.2 Mechanism and Key Parameters of Anchor Penetration

All previous researches describing the mechanism of the anchor penetration are based on the energy method (Neubecker and Randolph, 1996c) or the force method (LeLievre and Tabatabaee, 1979, 1981; Neubecker and Randolph, 1996b; Thorne, 1998). At any instantaneous embedment, the real movement direction must be the direction in which the soil resistance is easiest to be overcomed by the drag force. It is generally accepted that the instantaneous direction of the anchor movement is identical to the anchor orientation (Aubeny and Murff, 2005; Neubecker and Randolph, 1996a; O'Neill *et al*., 2003; Stewart, 1992; Thorne, 1998), which has been validated by both theoretical and experimental methods (Liu *et al*., 2012b). This motion characteristic forms the basis of the analytical model for the anchor positioning.

Based on the first and fourth assumptions in Section 2.1, as shown in Fig. 1, the process of the anchor penetration can be regarded as a two-dimensional motion. Therefore, throughout the anchor embedment, there are only three key position parameters, i.e., the horizontal position of the anchor x, the embedment depth of the anchor z (commonly referred to the center of anchor mass) and the anchor orientation θ_o. On the above motion characteristic, the following relation can be obtained as:

$$z_i - z_{i-1} = (x_i - x_{i-1}) \tan \theta_{oi}, \tag{1}$$

where, z_i and x_i are instantaneous position coordinates of the anchor, and θ_{oi} is the instantaneous anchor orientation. Besides, as shown in Fig. 3, according to the geometric relationship between the anchor orientation θ_o and the drag angle to the horizontal θ_{ah} at the shackle, at any penetration instant, the drag angle to the fluke at the shackle can be represented as:

$$\theta_a = \theta_o + \theta_{ah}. \tag{2}$$

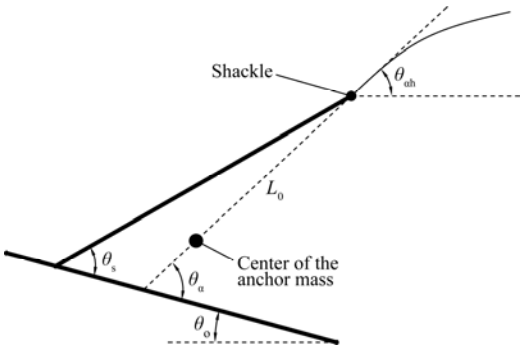

Fig. 3. Definition of the anchor fluke.

2.3 Mechanical Model for Drag Lines

The embedded anchor chain was analyzed by Neubecker and Randolph (1995), and an important expression of the chain tension at the point of attachment to the anchor pile was derived. The similar way is adopted for drag anchors to analyze the embedded line and then to derive the anchor positioning equations. Forces acting on the element of the embedded line are shown in Fig. 4.

In Fig. 4, T is the tension in the drag line; θ is the angle of the drag line to the horizontal; s is the distance measured along the drag line starting at the shackle; w is the submerged weight of the drag line per unit length; Q is the soil resistance normal to the drag line (per unit length of line); and F is the soil resistance tangential to the drag line (per unit length of line).

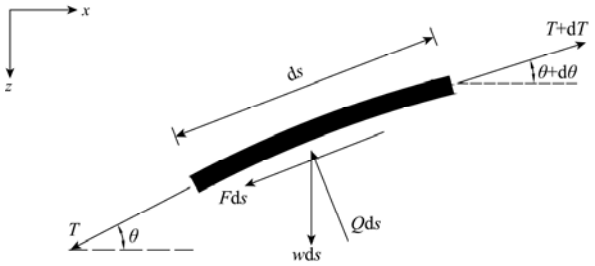

Fig. 4. Forces acting on an embedded line element.

On the basis of the force equilibriums both in the horizontal and vertical directions (Vivatrat *et al*., 1982) and introducing the relation $F = \mu Q$, the following differential equation can be obtained:

$$\frac{\mathrm{d}T}{\mathrm{d}s} + \mu T \frac{\mathrm{d}\theta}{\mathrm{d}s} = w(\sin\theta + \mu\cos\theta). \tag{3}$$

Ignoring the self weight of the drag line w, and only considering the force equilibrium in the vertical direction, Eq. (3) can be integrated to give the relation between the tension and soil resistance normal to the drag line:

$$T_{\mathrm{a}} \exp\left[\mu(\theta_{\mathrm{ah}} - \theta)\right] \frac{\mathrm{d}\theta}{\mathrm{d}s} = -Q, \tag{4}$$

where, T_{a} is the drag force at the shackle, and θ_{ah} is the drag angle to the horizontal at the shackle. By integrating Eq. (4) from the shackle to the embedment point along the embedded line and considering the initial embedment depth of the drag line ζ (Li, 2010), the following equation can be obtained:

$$\frac{T_{\mathrm{a}}}{1+\mu^2}\left[\exp(\mu\theta_{\mathrm{ah}}) - \cos\theta_{\mathrm{ah}} - \mu\sin\theta_{\mathrm{ah}}\right] = \int_{\zeta}^{z_{\mathrm{a}}} Q\mathrm{d}z, \tag{5}$$

where, z_{a} is the embedment depth of the shackle. From Eq. (5), the analytical expression can be easily obtained if the soil resistance Q is known. Obviously, the expressions of the soil resistance Q are different for cohesive and noncohesive soils.

In the saturated clay, the soil resistance Q is calculated by the Skempton's bearing capacity formula (Skempton, 1951):

$$Q = N_{cL} s_u b , \tag{6}$$

where, b is the effective bearing width of the embedded line, N_{cL} denotes the bearing capacity factor for the drag line, and s_u is the undrained shear strength which is generally represented as $s_u = s_{u0} + kz$, in which z is the soil depth below the seafloor surface, s_{u0} is the shear strength at the seafloor surface ($z = 0$), and k is the gradient of the undrained shear strength with depth. Based on the model tests, Degenkamp and Dutta (1989) proposed that $b = d$ and $b = 2.5d$ for cable and chain, respectively. For cable, d is the diameter; for chain, d is the nominal bar diameter. These recommended values are generally accepted (Neubecker and Randolph, 1996a; DNV, 2000; Miedema *et al*., 2007).

In saturated sand, the formula for the end bearing proposed by Terzaghi and Peck (1967) is adopted to calculate the normal soil resistance:

$$p = cN_c + qN_q + \frac{1}{2}\gamma t N_\gamma , \tag{7}$$

where, N_c, N_q and N_γ are the bearing capacity factors, c is the cohesion of soil, q is the uniformly distributed surcharge surrounding the footing, γ is the submerged unit weight of soil, and t is the thickness of the footing. Considering that the cohesion c in the saturated sand is approximately zero, and $\gamma t N_\gamma / 2$ is a small item related to qN_q, and then the first and third items in the right of Eq. (7) can be ignored. The surcharge q is related to the chain angle and can be expressed as:

$$q = \left(K_L \sin^2\theta + \cos^2\theta\right)\gamma z , \tag{8}$$

where, K_L is the lateral soil pressure factor for the drag line, which is related the vertical stress and the horizontal stress.

Because the chain angle varies along the embedded line, and it is actually unknown during penetration of the anchor, the applicability of Eq. (8) is limited. Therefore, an approximate expression with high precision that is independent of the chain angle is meaningful and derived with the following form:

$$q = \frac{1}{20}\left(3K_L + 17\right)\gamma z . \tag{9}$$

By substituting Eq. (9) into Eq. (7), the soil resistance Q can be represented as:

$$Q = \frac{1}{20}\left(3K_L + 17\right)\gamma z N_{qL} b , \tag{10}$$

where N_q is replaced with N_{qL} that denotes the bearing capacity factor for the drag line. Finally, substituting Eq. (6) or Eq. (10) into Eq. (5), and introducing the relation between the embedment depth of the mass center of the anchor and the shackle, i.e., $z_c = z_a + L_0 \sin\theta_{ah}$, then, the relationship among z_c, θ_{ah} and T_a both for cohesive and noncohesive soils can be uniformly expressed as:

$$F_1\left(z_c, \theta_{ah}, T_a\right) = 2T_a\left[\exp(\mu\theta_{ah}) - \cos\theta_{ah} - \mu\sin\theta_{ah}\right] - bf_1\left(z_c\right)\left(1+\mu^2\right) = 0 , \tag{11}$$

where, z_c is the embedment depth of the mass center of the anchor, L_0 is the distance from the shackle

to the mass center of the anchor, and $f_1(z_c)$ is the function of z_c that is related to the drag line and soil properties, as listed in Table 1.

Table 1 Coefficients in Eqs. (11) and (14)

	Sand		Clay
	Exact expression	Simplified expression	
$f_1(z_c)$	$\frac{1}{20}(3K_L+17)N_{qL}\gamma\left[(z_c-L_0\sin\theta_{ah})^2-\zeta^2\right]$		$2N_{cL}s_{u0}(z_c-L_0\sin\theta_{ah}-\zeta)$ $+N_{cL}k\left[(z_c-L_0\sin\theta_{ah})^2-\zeta^2\right]$
$f_2(z_c)$	$(K_1A_{sn}+K_2A_b+K_3A_{sm})\gamma z_c$		$(N_{cf}A_b+\alpha_f A_s)(s_{u0}+kz_c)$
K_1	$K_f\tan\delta_f$		–
K_2	$K_f\cos^2\theta_o+\sin^2\theta_o$	$\frac{1}{20}(17K_f+3)N_{qf}$	–
K_3	$(K_f\sin^2\theta_o+\cos^2\theta_o)\tan\delta_f$	$\frac{1}{20}(3K_f+17)\tan\delta_f$	–

It is noted that the value of the frictional coefficient μ in sand is usually different from that in clay. In sand, $\mu=\tan\delta_1$ is widely used, in which δ_1 denotes the angle of interface friction for the drag line. In clay, it is suggested by Neubecker and Randolph (1995) and Li (2010) that the value of μ for chain is 0.4–0.6 and 0.1–0.6, respectively. The value of the frictional coefficient is also different for chain and cable. Usually the value of μ for chain is larger than that for cable. It is suggested by DNV (2000) that the value of μ be 0.6−0.8 and 0.1−0.3 for chain and cable in clay, respectively.

The initial embedment depth of the drag line ζ can be evaluated based on the previous work (Li, 2010). For the clay with a uniform strength, ζ=0 ; for the clay with a linear strength, $\zeta=w/(kN_{cL}b)-s_{u0}/k$ and $\zeta\geq 0$; for the noncohesive soil, $\zeta=w/(N_{qL}\gamma b)$.

2.4 Mechanical Model for Drag Anchors

The mechanical model for a drag anchor developed by Liu *et al*. (2012b) is adopted in the present work, as illustrated in Fig. 5. For the purpose of concise expression, the details will not be repeated here. Only the important conclusions are presented as follows.

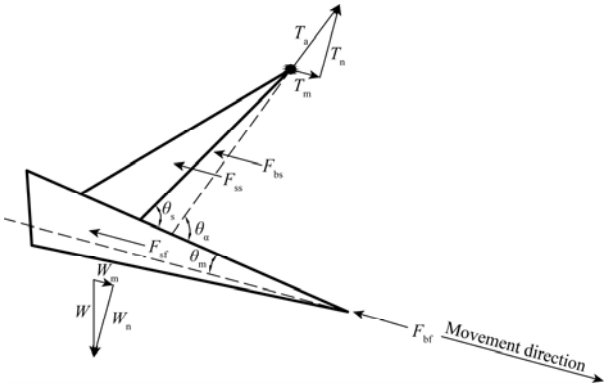

Fig. 5. Mechanical model of a drag anchor.

According to the force equilibrium in the movement direction, we can obtain:

$$T_{\mathrm{a}}\cos\left(\theta_{\mathrm{a}}-\theta_{\mathrm{m}}\right)-F_{\mathrm{b}}-F_{\mathrm{s}}+W\sin\left(\theta_{\mathrm{o}}-\theta_{\mathrm{m}}\right)=0\,, \tag{12}$$

where, θ_{a} denotes the drag angle to the fluke at the shackle; θ_{o} denotes the fluke orientation to the horizontal; and θ_{m} denotes the angle of the movement direction to the top surface of the fluke; F_{b} and F_{s} are defined as the total end bearing and total shear force in the movement direction on the anchor, respectively; W denotes the submerged anchor weight. In Fig. 5, T_{m} and T_{n} are components of T_{a} in the movement direction and the normal to the movement direction, respectively; W_{m} and W_{n} are components of W in the movement direction and the normal to the movement direction, respectively; F_{bf} and F_{bs} are end bearings in the movement direction on the fluke and the shank, respectively; F_{sf} and F_{ss} are shear forces in the movement direction on the fluke and the shank, respectively.

In saturated clay, F_{b} and F_{s} can be represented as:

$$\begin{cases} F_{\mathrm{b}}=N_{\mathrm{cf}}s_{\mathrm{u}}A_{\mathrm{b}} \\ F_{\mathrm{s}}=\alpha_{\mathrm{f}}s_{\mathrm{u}}A_{\mathrm{s}} \end{cases} \tag{13a}$$

where N_{cf} denotes the bearing capacity factor for the anchor, α_{f} denotes the adhesion factor for the anchor, A_{b} is the effective bearing area of the anchor, which is the total projected area of the anchor (including the shank and fluke) on to the plane perpendicular to the movement direction, and A_{s} is the effective shear area of the anchor, which is the total shear area of the anchor (including the shank and fluke) along the movement direction.

In saturated sand, if adopting the exact expressions of surcharge q and shear stress τ, F_{b} and F_{s} are represented as:

$$\begin{cases} F_{\mathrm{b}}=(K_{\mathrm{f}}\cos^2\theta_{\mathrm{o}}+\sin^2\theta_{\mathrm{o}})\gamma z_{\mathrm{c}}N_{\mathrm{qf}}A_{\mathrm{b}} \\ F_{\mathrm{s}}=[(K_{\mathrm{f}}\sin^2\theta_{\mathrm{o}}+\cos^2\theta_{\mathrm{o}})A_{\mathrm{sm}}+K_{\mathrm{f}}A_{\mathrm{sn}}]\gamma z_{\mathrm{c}}\tan\delta_{\mathrm{f}} \end{cases} \tag{13b}$$

If adopting the simplified expressions of surcharge q and shear stress τ, Eq. (13b) is simplified to:

$$\begin{cases} F_{\mathrm{b}}=\dfrac{1}{20}\left(17K_{\mathrm{f}}+3\right)\gamma z_{\mathrm{c}}N_{\mathrm{qf}}A_{\mathrm{b}} \\ F_{\mathrm{s}}=\left[\dfrac{1}{20}\left(3K_{\mathrm{f}}+17\right)A_{\mathrm{sm}}+K_{\mathrm{f}}A_{\mathrm{sn}}\right]\gamma z_{\mathrm{c}}\tan\delta_{\mathrm{f}} \end{cases} \tag{13c}$$

where, K, N_{q}, δ, and z are replaced with K_{f}, N_{qf}, δ_{f}, and z_{c}, which denote the lateral soil pressure factor for the anchor, the bearing capacity factor for the anchor, the angle of interface friction for the anchor, and the embedment depth of the mass center of the anchor, respectively. If the plane which the anchor moves along is defined as the primary plane of the anchor and represents the fluke orientation, and then A_{sm} denotes the effective shear area of the anchor projected to the primary plane of the fluke, and A_{sn} denotes the effective shear area of the anchor projected to the plane perpendicular to the primary plane and along the movement direction of the fluke.

By substituting Eq. (13) into Eq. (12), the relationship among z_c, θ_a, θ_{ah} and T_a for cohesive and noncohesive soils can be uniformly represented as:

$$F_2\left(z_c,\theta_a,\theta_{ah},T_a\right)=T_a\cos\left(\theta_a-\theta_m\right)-f_2\left(z_c\right)+W\sin\left(\theta_a-\theta_{ah}-\theta_m\right)=0, \tag{14}$$

where $f_2\left(z_c\right)$ denotes the function of z_c that is related to the anchor and soil properties. The expressions of $f_2\left(z_c\right)$ are different for cohesive and noncohesive soils, as listed in Table 1.

2.5 Theoretical Relationship Between the Embedment Depth and the Anchor Orientation

Because the anchor line tension equals the anchor pullout resistance at the shackle, by combining Eqs. (11) and (14), and introducing Eq. (2), the following expression can be obtained:

$$\begin{aligned}F\left(z_c,\theta_o\right)=&b\left(1+\mu^2\right)\cos\left(\theta_a-\theta_m\right)f_1\left(z_c\right)\\&-2\left\{\exp\left[\mu(\theta_a-\theta_o)\right]-\cos\left(\theta_a-\theta_o\right)-\mu\sin\left(\theta_a-\theta_o\right)\right\}\left[f_2\left(z_c\right)-W\sin\left(\theta_o-\theta_m\right)\right]=0.\end{aligned} \tag{15}$$

Eq. (15) is the theoretical relationship between the embedment depth and the anchor orientation; and by combining Eq. (1), the anchor positioning equations have been initially established. From Eq. (15), it can be found that, under a specific condition, i.e., the anchor, drag line and soil properties are known, and the movement direction θ_m can be determined by the theoretical method proposed by Liu *et al*. (2012b). The problems now remaining are: what is the property of the drag angle at the shackle θ_a? Is it a constant during penetration and which constant will it be? If not a constant, how does it vary with the embedment depth? If all these problems related to the drag angle at the shackle are clarified, then the anchor positioning equations can be solved ultimately.

3. Drag Angle at the Shackle

3.1 Analytical Method for Determining the Drag Angle at the Shackle

An analytical method for determining both the variation of θ_a with the embedment depth and the value of θ_a for a general drag anchor, including both the Stevmanta and Dennla VLAs that are the main two commercial drag anchors, is developed in this section, which is based on the assumption that the direction of the drag force at the shackle passes through the mass center of the anchor during the dragging process. There are two considerations supporting this assumption. Firstly, from a macroscopic scale, the drag anchor embedded in soils can be looked as a mass point and the end point of the embedded line. Therefore, all forces acting on the anchor pass through the mass center of the anchor. Secondly, for the purpose of practical application, during the anchor embedment, there will be a better balance between the penetration efficiency and stability of the anchor if the direction of the drag force at the shackle passes through the mass center of the anchor. As demonstrated in Fig. 6, the forces acting on the anchor include the drag force at the shackle T_a, the total soil resistance R, and the submerged anchor weight W; CM, CM_f and CM_s denote the mass centers of the anchor, the fluke and the shank, respectively; $\left(x_m,y_m\right)$, $\left(x_f,y_f\right)$, $\left(x_s,y_s\right)$ and $\left(x_{shackle},y_{shackle}\right)$ are the position coordinates of CM, CM_f, CM_s and the shackle, respectively; m_f and m_s are the masses of the fluke and the shank,

respectively; L_1 denotes the distance from CM_f to the shank-fluke attachment point, and L_s denotes the length of the shank.

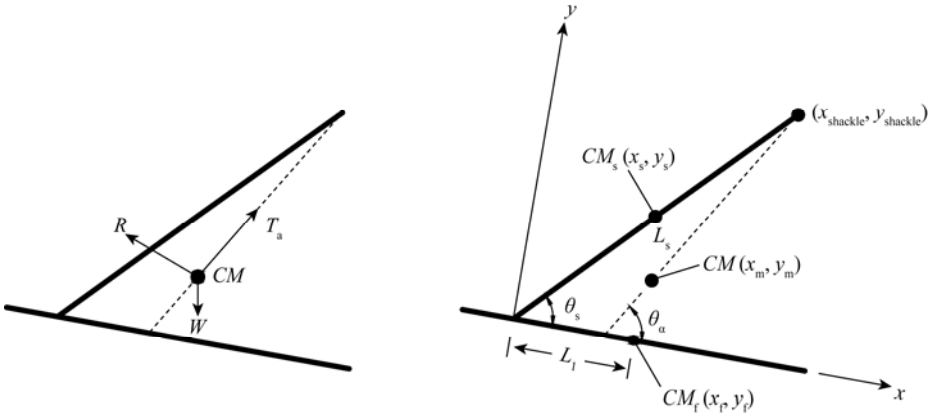

(a) Forces acting on the anchor (b) Mass centers of the fluke, shank and anchor

Fig. 6. Geometry of a drag anchor.

The position coordinates of CM_f, CM_s and the shackle in the local coordinate system can be expressed as:

$$\begin{cases} x_f = L_1; \quad y_f = 0 \\ x_s = \dfrac{1}{2} L_s \cos\theta_s; \quad y_s = \dfrac{1}{2} L_s \sin\theta_s \\ x_{shackle} = L_s \cos\theta_s; \quad y_{shackle} = L_s \sin\theta_s \end{cases} \tag{16}$$

Then, according to the geometric property of the anchor, the position coordinates of CM can be expressed as:

$$\begin{cases} x_m = \dfrac{m_f x_f + m_s x_s}{m_f + m_s} = \dfrac{2m_f L_1 + m_s L_s \cos\theta_s}{2\left(m_f + m_s\right)} \\ y_m = \dfrac{m_f y_f + m_s y_s}{m_f + m_s} = \dfrac{m_s L_s \sin\theta_s}{2\left(m_f + m_s\right)} \end{cases} \tag{17}$$

Considering the previous assumption and the geometry again, the drag angle at the shackle θ_a can be expressed as:

$$\theta_a = \arctan\left(\frac{y_{shackle} - y_m}{x_{shackle} - x_m}\right) = \arctan\left[\frac{\left(2 + m_s/m_f\right)\sin\theta_s}{\left(2 + m_s/m_f\right)\cos\theta_s - 2L_1/L_s}\right], \quad 0 < \theta_a < \pi/2 . \tag{18}$$

It is observed from Eq. (18) that the value of θ_a can be solved if either of the two conditions is known, i.e., the position coordinates of CM and the shackle, or the anchor properties including θ_s, m_s / m_f and L_1 / L_s. Furthermore, it is clear that, for a specific drag anchor, the parameters of the anchor property are known. Therefore, the value of θ_a is known, and it can be concluded that the drag angle at

the shackle θ_a is a constant during penetration and it does not vary with the embedment depth.

3.2 Comparative Study

In order to examine the analytical method for predicting the drag angle at the shackle, all the available data reported in literatures are collected for calculation and comparison. As listed in Table 2, the data are divided into two categories according to the two conditions mentioned in the end of Section 3.1. There are four simple anchor models with different sizes used by Murff *et al.* (2005); one simple anchor model used by Ruinen (2004) in numerical modelling; three simplified anchor models whose prototypes are the Bruce anchors adopted by Kim (2005) in numerical modelling; two scale models of a Vryhof Stevpris 32t anchor in the centrifuge tests adopted by O'Neill and Randolph (2001); three rectangular models with flexible shanks employed in the model flume experiments by Liu *et al*. (2010). Based on the known data of the anchor models, the necessary data for using Eq. (18) can be obtained, and then the value of θ_a can be calculated. In Table 2, θ_a' denotes the value of θ_a reported in the literature, which is determined through either the numerical simulation or the experiment.

Table 2 Anchor properties and prediction results of the drag angle at the shackle

Anchor property	Murff *et al*.				Kim
	1	2	3	4	1
(x_m, y_m)	(0.83, 0.22)	(0.89, 0.42)	(0.64, 0.22)	(0.88, 0.16)	(2.19, 1.51)
$(x_{shackle}, y_{shackle})$	(2.50, 2.98)	(2.50, 2.98)	(2.50, 2.98)	(3.19, 2.23)	(5.53, 6.59)
θ_s (º)	50.0	50.0	50.0	35.0	50.0
θ_a (º)	58.7	57.8	56.0	41.9	56.7
$\theta_a - \theta_s$ (º)	8.7	7.8	6.0	6.9	6.7

Anchor property	Kim		O'Neill and Randolph		Ruinen	Liu *et al*.		
	2	3	1	2	1	1	2	3
m_s / m_f	0.040	0.039	0.608	0.617	0.208	0	0	0
L_l / L_s	0.091	0.047	0.148	0.100	0.108	0	0	0
θ_s (º)	50.0	65.0	32.0	50.0	50.0	24.0	29.5	33.3
θ_a' (º)	–	73.0	–	–	56.4	24.0	29.5	33.3
θ_a (º)	54.1	67.6	32.5	49.3	54.5	24.0	29.5	33.3
$\lvert\theta_a - \theta_a'\rvert$	–	5.4	–	–	1.9	0	0	0
$\theta_a - \theta_s$ (º)	4.1	2.6	0.5	-0.7	4.5	0	0	0

It is observed from Table 2 that, for the drag anchor with rigid shanks (except the models used by Liu *et al.*, 2010), such as the conventional drag anchors and the Dennla VLAs, nearly all the values of θ_a are larger than those of the shank angle θ_s, and the difference ranges from 0.5º to 8.7º; for the drag anchor with flexible shanks, such as the Stevmanta VLAs, the value of θ_a exactly equals that of the shank angle θ_s. Compared with the known value of θ_a, the maximum deviation of the predicted angles is 5.4º, and other deviations are smaller than 1.9º. In conclusion, the predicted results match with our knowledge of the drag angle at the shackle for the anchor with either rigid or flexible shanks.

Until now, all the unknown variables in Eq. (15) have been clarified. By utilizing Eqs. (1), (15) and (18), the anchor positioning equations can be finally established by the following set of equations:

$$\begin{cases} \theta_{\mathrm{a}} = \arctan\left(\dfrac{y_{\mathrm{shackle}} - y_{\mathrm{m}}}{x_{\mathrm{shackle}} - x_{\mathrm{m}}}\right) = \arctan\left[\dfrac{\left(2 + m_{\mathrm{s}}/m_{\mathrm{f}}\right)\sin\theta_{\mathrm{s}}}{\left(2 + m_{\mathrm{s}}/m_{\mathrm{f}}\right)\cos\theta_{\mathrm{s}} - 2L_{\mathrm{l}}/L_{\mathrm{s}}}\right], \quad 0 < \theta_{\mathrm{a}} < \pi/2 \\ F\left(z_{\mathrm{c}}, \theta_{\mathrm{o}}\right) = b\left(1+\mu^2\right)\cos\left(\theta_{\mathrm{a}} - \theta_{\mathrm{m}}\right) f_{\mathrm{l}}\left(z_{\mathrm{c}}\right) \\ \qquad\qquad - 2\left[\mathrm{e}^{\mu(\theta_{\mathrm{a}} - \theta_{\mathrm{o}})} - \cos\left(\theta_{\mathrm{a}} - \theta_{\mathrm{o}}\right) - \mu\sin\left(\theta_{\mathrm{a}} - \theta_{\mathrm{o}}\right)\right]\left[f_2\left(z_{\mathrm{c}}\right) - W\sin\left(\theta_{\mathrm{o}} - \theta_{\mathrm{m}}\right)\right] = 0 \\ z_{\mathrm{i}} - z_{\mathrm{i-1}} = \left(x_{\mathrm{i}} - x_{\mathrm{i-1}}\right)\tan\theta_{\mathrm{oi}} \end{cases} \tag{19}$$

In Eq. (19), firstly, the exact value of θ_{a} can be deduced by the first equation; then, the relation between z_{c} and θ_{o} can be obtained by the second equation; finally, the position of the anchor during the whole anchor embedment process can be deduced by the third incremental formula. In order to obtain a reasonable result, the restrictive conditions are used as follows:

$$\begin{cases} \mathrm{d}\theta_{\mathrm{o}}/\mathrm{d}z_{\mathrm{c}} < 0 \\ \mathrm{d}\left(\theta_{\mathrm{a}} - \theta_{\mathrm{o}}\right)/\mathrm{d}z_{\mathrm{c}} > 0 \\ 0 \le \theta_{\mathrm{o}} \le \theta_{\mathrm{a}} \end{cases} \tag{20}$$

4. Comparison Between Analytical Predictions and Model Tests

In order to examine the anchor positioning equations, i.e., Eq. (19), specially designed experiments were carried out in a model experimental system. The model experimental system mainly consists of four parts, i.e., the experimental flume, the drag and retrieval system, the measurement system, and the drag-mooring conversion system. Through the experimental system, dynamic and motion parameters of the anchor, including the trajectory, drag force, drag distance, drag angle at the shackle, and pitch together with the roll of the anchor model, can be gathered and simulated simultaneously. Details of the experimental system including the technique for measuring the anchor trajectory in soils can be found in the references (Liu *et al*., 2010; Zhang *et al*., 2011). Main parameters of the anchor models are presented in Table 3, in which d_{s} is the diameter of the soft cable shank, s_{s} is the lateral distance between the cable shanks, and L_0 is the distance from the shackle to the center of the anchor mass. The sand parameters are listed in Table 4. The diameter and length of the drag line are 6 mm and 7000 mm, respectively. All test cases can be found in Table 5.

By employing a recently developed technique, the anchor trajectories in soils are measured with high precision (Zhang *et al*., 2011), as presented in Fig. 7. Completely following the test cases, theoretical predictions of the anchor position at every instantaneous embedment depth during dragging by employing the anchor positioning equations can be obtained and are also presented in Fig. 7. The parameters including the bearing capacity factor N_{q}, the lateral soil pressure factor K, and the angle of interface friction δ are obtained through the recent study (Zhang, 2011), i.e., $N_{\mathrm{qf}} = 27$, $N_{\mathrm{qL}} = 23$; $K_{\mathrm{f}} = K_{\mathrm{L}} = 1.2$; and $\delta_{\mathrm{f}} = 30°$, $\delta_{\mathrm{L}} = 28°$. According to the theoretical method established by references (Zhang, 2011; Liu *et al*., 2012b), for the anchor with a rectangular fluke section, the penetration direction of the anchor in soils parallels the fluke surface, i.e., $\theta_{\mathrm{m}} = 0°$. Besides, owing to the anchor models designed for experiments are square plate anchors with flexible shanks, by adopting the analytical

method established in Section 3.1, the value of θ_a has been deduced equally to θ_s by using the first equation in Eq. (19), as listed in Table 5. For sand, the initial embedment depth of the drag line $\zeta = 0.8$ mm is directly measured.

Table 3 Main parameters of the anchor models

Anchor	Rectangular		
	Small	Middle	Large
Length (m)	0.20	0.25	0.30
Tip length (m)	0.0500	0.0625	0.0750
Width (m)	0.20	0.25	0.30
Thickness (m)	0.012	0.014	0.016
Weight (kN)	0.036	0.058	0.110
d_s (m)	0.003	0.003	0.003
s_s (m)	0.100	0.125	0.150
L_0 (m)	0.24	0.30	0.36

Table 4 Parameters of sand

Density (kg/m^3)	Max. density (kg/m^3)	Min. density (kg/m^3)	Relative density	Dry unit weight (kN/m^3)	Internal friction angle (°)	Natural angle of repose (°)
1624	1730	1480	0.6	15.9	34	32

Table 5 Cases and parameters in the verification with model tests

Case	1	2	3	4	5	6	7	8	9
Model	Small			Middle			Large		
θ_s (°)	24.0	29.5	33.3	24.0	29.5	33.3	24.0	29.5	33.3
θ_a (°)	24.0	29.5	33.3	24.0	29.5	33.3	24.0	29.5	33.3
A_b (m^2)	0.0050	0.0052	0.0053	0.0063	0.0066	0.0068	0.0084	0.0087	0.0089
A_s (m^2)	0.1272	0.1269	0.1267	0.1701	0.1698	0.1696	0.2411	0.2407	0.2404

In Fig. 7, the vertical dashed line in each figure denotes the embedment position of anchor where the distance between the fluke and the end wall of the flume is 3B. The measured data exceeding the dashed line are considered to be affected by side effects because of the limitation of the size of the experimental flume. It means that only the measured data before the dashed line can be reliably compared with the theoretically predicted trajectories. It is observed that, except in Cases 1, 4 and 7, the general agreement between measured and predicted trajectories is satisfied. Considering that Cases 1, 4 and 7 represent a very shallow embedment (the ultimate embedment depth are smaller than B), on one hand, the top soil is easily disturbed during the model test, on the other hand, the effect of the drag line is more remarkable at a very shallow embedment of the anchor, these factors may impair the reasonable comparison between the predicted and measured data. Above all, it is concluded that the analytical method can well simulate the measured data.

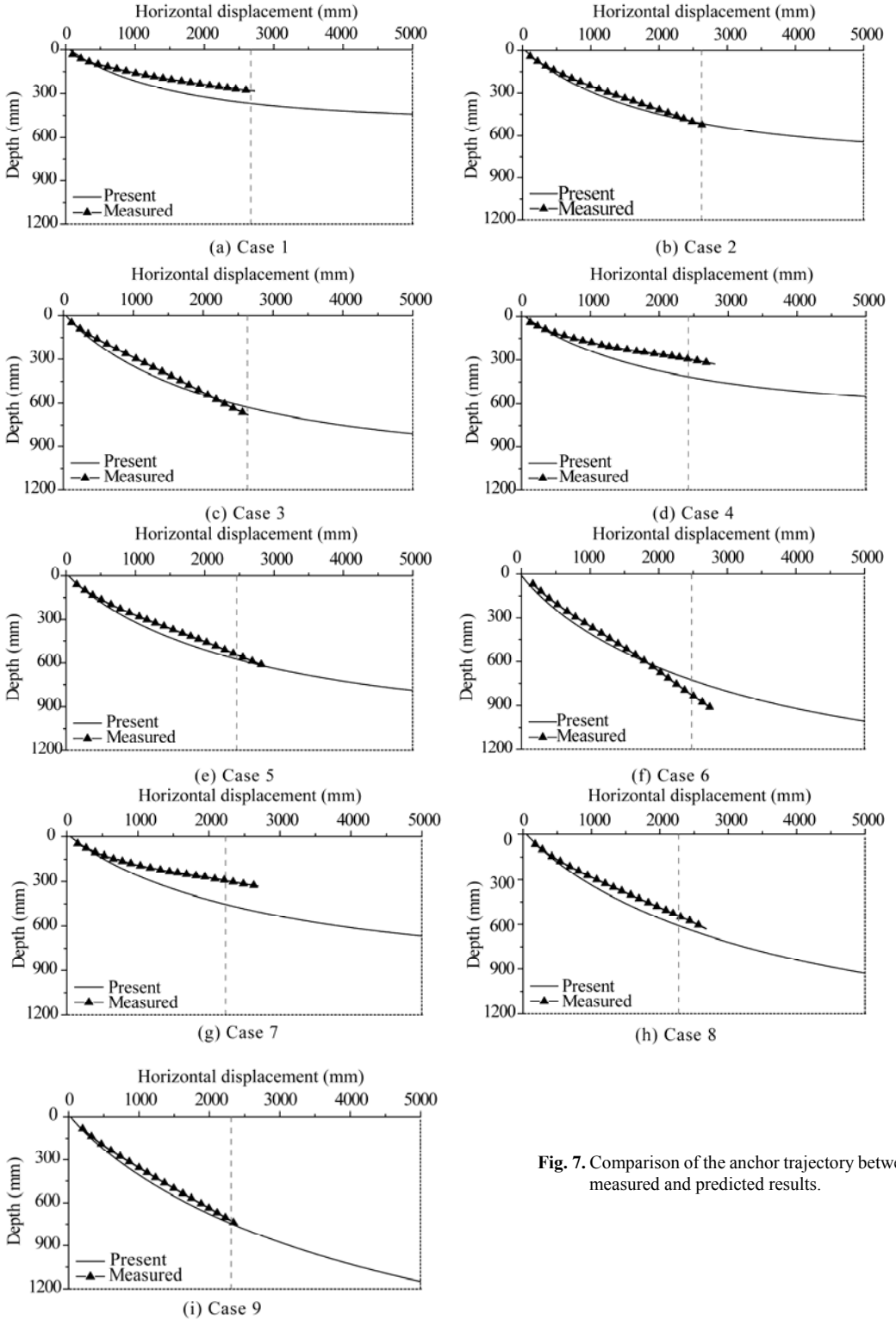

Fig. 7. Comparison of the anchor trajectory between measured and predicted results.

5. Concluding Remarks

In this paper, a novel theoretical framework for positioning drag anchors both in cohesive and noncohesive soils with either uniform or linear strengths has been well established. The proposed model is based on the mechanical models and mathematical derivations, which can be applicable to not only small scale models in laboratory tests but also full-size anchors in the field tests. Through the positioning theoretical model and theoretical framework, more information and many concepts related to the drag embedment problem have been gained and described, such as the properties of the embedded segment of the installation line; the anchor behaviors including the anchor position, anchor orientation and movement direction; the interaction between the anchor and the installation line, and so on. More importantly, analytical methods for determining the value of the drag angle at the shackle have already been founded through the present study. The general hypothesis of the drag angle adopted by many investigators has been confirmed, and this study proves that the drag angle at the shackle during penetration keeps constant and independent of the anchor and soil properties except the shank angle of the anchor. The positioning method for drag anchors which considers the interaction between the drag anchor and the installation line provides a reasonable theoretic approach to investigate the anchor behaviors in soils. By comparing with the model flume experiments, the sensitivity, effectiveness and veracity of the method for positioning drag anchors have been well verified.

However, positioning drag anchors is quite complex in the practical engineering, and it is controlled by many factors, such as installation techniques, seafloor terrain, properties of the anchor and seabed soils. How to improve both the prediction accuracy and analytical model deserves further study.

Acknowledgements – The authors would like to thank Mr. ZHAO Yanbing, Ms. HU Cun, Mr. LIU Chenglin, Mr. HUANG Wei and Mr. YUE Yanzhao, for their generous help with the experiments and calculations.

References

Aubeny, C. P., Kim, B. M. and Murff, J. D., 2005. Proposed upper bound analysis for drag embedment anchors in soft clay, *Proc. Int. Symp. Front. Offshore Geotech., ISFOG 2005*, London, Taylor & Francis Group, 179−183.

Aubeny, C. P. and Murff, J. D., 2005. *Suction Caissons and Vertical Loaded Anchors: Design Analysis Method*, Final Report, Texas A & M University.

Aubeny, C. P., Murff, J. D. and Kim, B. M., 2008. Prediction of anchor trajectory during drag embedment in soft clay, *Int. J. Offshore Polar Eng.*, **18**(4): 314−319.

Dahlberg, R., 1998. Design procedures for deepwater anchors in clay, *Proc. 30th Annual Offshore Tech. Conf.*, Houston, OTC 8837.

Degenkamp, G. and Dutta, A., 1989. Soil resistances to embedded anchor chain in soft clay, *J. Geotech. Eng.*, **115**(10): 1420−1438.

Det Norshke Veritas (DNV), 2000. *Design and Installation of Fluke Anchors in Clay*, DNV RP E301, Oslo, Det Norshke Veritas.

Kim, B. M., 2005. *Upper Bound Analysis for Drag Anchors in Soft Clay*, Ph. D. Thesis, Texas A & M University.

LeLievre, B. and Tabatabaee, J., 1979. Holding capacity of marine anchors in sand, *Proceedings of the 1st Canadian Conference on Marine Geotechnical Engineering*, Calgary, 301−311.

LeLievre, B. and Tabatabaee, J., 1981. The performance of marine anchors with planar flukes in sand, *Can. Geotech.*

J., **18**(4): 520−534.

Li, Y., 2010. *Reverse Catenary Equations of Drag Lines and Application to the Kinematic Model of Drag Anchors*, M. S. Thesis, Tianjin University. (in Chinese)

Liu, H. X., Zhang, W., Zhang, X. W. and Liu, C. L., 2010. Experimental investigation on the penetration mechanism and kinematic behavior of drag anchors, *Appl. Ocean Res.*, **32**(4): 434−442.

Liu, H. X., Liu, C. L., Yang, H. T., Li, Y., Zhang, W. and Xiao, Z. J., 2012a. A novel kinematic model for drag anchors in seabed soils, *Ocean Eng.*, **49**, 33−42.

Liu, H. X., Zhang, W., Liu, C. L. and Hu, C., 2012b. Movement direction of drag anchors in seabed soils, *Appl. Ocean Res.*, **34**, 78−95.

Miedema, S. A., Lagers, G. H. G. and Kerkvliet, J., 2007. An overview of drag embedded anchor holding capacity for dredging and offshore applications, *Proceedings of the 18th World Dredging Congress*, Orlando, 1−28.

Murff, J. D., Randolph, M. F., Elkhatib, S., Kolk, H. J., Ruinen, R. M., Strom, P. J. and Thorne, C. P., 2005. Vertically loaded plate anchors for deepwater applications, *Proceedings of International Symposium on Frontiers in Offshore Geotechnics*, *ISFOG 2005*, London, Taylor & Francis Group, 31−48.

Naval Civil Engineering Laboratory (NCEL), 1987. *Drag Embedment Anchors for Navy Moorings*, Techdata Sheet 83-08R (NCEL 83-08R), California, USA.

Neubecker, S. R. and Randolph, M. F., 1995. Profile and frictional capacity of embedded anchor chains, *J. Geotech. Eng.*, **121**(11): 797−803.

Neubecker, S. R. and Randolph, M. F., 1996a. The performance of drag anchor and chain system in cohesive soil, *Mar. Geores. Geotechnol.*, **14**(2): 77−96.

Neubecker, S. R. and Randolph, M. F., 1996b. The static equilibrium of drag anchors in sand, *Can. Geotech. J.*, **33**(4): 574−583.

Neubecker, S. R. and Randolph, M. F., 1996c. The kinematic behavior of drag anchors in sand, *Can. Geotech. J.*, **33**(4): 584−594.

O'Neill, M. P. and Randolph, M. F., 2001. Modelling drag anchors in a drum centrifuge, *Int. J. Phys. Model Geotech.*, **1**(2): 29−41.

O'Neill, M. P., Bransby, M. F. and Randolph, M. F., 2003. Drag anchor fluke-soil interaction in clays, *Can. Geotech. J.*, **40**(1): 78−94.

Ruinen, R. M., 2004. Penetration analysis of drag embedment anchors in soft clay, *Proc. 14th Int. Offshore Polar Eng. Conf.*, ISOPE, Toulon, 531−537.

Skempton, A. W., 1951. The bearing capacity of clays, *Proceedings of the Building Research Congress*, London, 180−189.

Stewart, W. P., 1992. Drag embedment anchor performance prediction in soft soils, *Proc. 24th Annual Offshore Tech. Conf.*, Houston, OTC 6970.

Terzaghi, K. and Peck, R. B., 1967. *Soil Mechanics in Engineering Practice*, Hoboken, John Wiley and Sons.

Thorne, C. P., 1998. Penetration and load capacity of marine drag anchors in soft clay, *J. Geotech. Geoenviron. Eng.*, **124**(10): 945−953.

Vivatrat, V., Valent, P. J. and Ponterio, A. A., 1982. The influence of chain friction on anchor pile design, *Proc. 14th Annual Offshore Tech. Conf.*, Houston, 153−163.

Vryhof Anchors, 2005. *Anchor Manual*, Zuid-Holland, Krimpen ad Yssel.

Zhang, W., 2011. *Penetration Mechanism and Kinematic Behavior of Drag Anchor*, Ph. D. Thesis, Tianjin University.

Zhang, W., Liu, H. X., Zhou, H. F. and Sheng, Z. G., 2011. A new technique to measure the trajectory of drag anchors in soils, *Geotech. Test. J.*, **34**(4): 279−287.